Electromagnetics, 26:175–187, 2006

ISSN: 0272-6343 print/1532-527X online
DOI: 10.1080/02726340500486492

Taylor & Francis
Taylor & Francis Group

Computation of the Electromagnetic Modes in Two-Dimensional Photonic Crystals: A Technique to Improve the Convergence Rate of the Plane Wave Method

MÁRIO G. SILVEIRINHA

Electrical Engineering Department—Instituto de Telecomunicações
Pólo II da Universidade de Coimbra
Coimbra, Portugal

CARLOS A. FERNANDES

Instituto Superior Técnico—Instituto de Telecomunicações
Technical University of Lisbon
Lisbon, Portugal

In this article, a regularization technique that allows the computing of the electromagnetic Floquet solutions in two-dimensional photonic crystals using a modified plane wave approach with very good convergence rate is described. The idea is to map the original electromagnetic fields into a space of smooth functions. This work is a generalization of a method previously proposed by the authors for metallic crystals, and the formulation presented here allows the characterizing of two-phase dielectric crystals. The numerical results show that the efficiency of our method is dramatically superior to that of the standard plane wave method.

Keywords photonic band gap, photonic crystals, plane wave method

Introduction

Photonic crystals are periodic dielectric/metallic structures. At the end of the 1980s, Yablanovitch (1987) hinted that if these structures were properly designed, the propagation of electromagnetic waves could be rigorously forbidden. Later, experimental results and numerical simulations proved that this conjecture was correct and that photonic crystals may have omnidirectional band gaps (Yablonovitch, Gmitter, & Leung, 1991). An important property of photonic crystals is that defects introduced intentionally in the periodic lattice (i.e., addition or removal of dielectric material) can give rise to localized

Received 5 July 2004; accepted 27 October 2004.
This work was funded by Fundação para Ciência e a Tecnologia under project POSI 34860/99.
Address correspondence to Mário G. Silveirinha, Electrical Engineering Department—Instituto de Telecomunicações, Polo II da Universidade de Coimbra, 3030 Coimbra, Portugal. E-mail: mario.silveirinha@co.it.pt

electromagnetic modes (Meade et al., 1991). This can be used to make high-Q cavities and waveguides with sharp bends that confine the light losslessly at short wavelengths (Yablonovitch, Gmitter, Meade, et al., 1991; Sakoda, 2001). Other novel phenomena and applications have been reported over the years. Remarkable examples are the superprism effect and negative refraction resulting from highly anisotropic dispersion curves (Luo et al., 2002; Kosaka et al., 1998). The application of the band gap concept to the microwave and (sub)millimeter wave bands has also been the subject of intensive study. A review of the state of the art is presented in Maagt et al. (2003).

The characterization of the electromagnetic modes of a photonic crystal is computationally very intensive. In previous work, the authors of this paper proposed a new hybrid method to compute efficiently the band structure of metallic crystals (Silveirinha & Fernandes, 2003, 2004). The idea is to map the electromagnetic eigenmodes into a space of "smooth functions" and to formulate an equivalent eigenvalue problem in the new space. The eigenvalue problem in the transformed space can then be efficiently solved using the plane wave method, because the transformed eigenmodes are smooth and so they can be expanded into a fast-converging Fourier series.

The objective of this paper is to explain how the method can be extended to dielectric crystals. The main difficulty in treating the dielectric case is to get rid of the discontinuities of the dielectric medium. To this end, we will unfold the original problem into two coupled propagation problems in homogeneous spaces. This procedure has no analogue in our previous works (Silveirinha & Fernandes, 2003, 2004) on metallic crystals. For simplicity, it is assumed that the photonic crystal is two-dimensional, i.e., that the inclusions have cylindrical symmetry.

The standard plane wave method is inefficient because the electromagnetic fields are discontinuous at the dielectric interfaces and thus the plane wave expansions converge very slowly (Walker, 1988). This problem is particularly serious when the dielectric contrast is high or when the electrical distance between the inclusions is small (Sozuer & Haus, 1993; Sozuer, Haus, & Inguva, 1992; Villeneuve & Piché, 1994). Sometimes the computational resources may even be insufficient to reach convergence (Villeneuve & Piché, 1994; Meade et al., 1993). The objective of our method is precisely to avoid this situation. To this end, and in analogy with the metallic problem, the electromagnetic modes are mapped into a space of smooth functions. It will be shown that the convergence rate of the method proposed here is dramatically superior to that of the standard plane wave method.

The outline of the article is as follows. First, the geometry and the formulation of the method will be described. Both polarization cases are studied, and on-plane propagation is assumed. Then, we will present numerical simulations that validate the theory and show the excellent convergent rate of the approach described here. Finally, conclusions will be drawn.

Dielectric Crystals

Here, it is explained how the method developed in Silveirinha and Fernandes (2003) can be generalized to the dielectric case. The main difficulty is to get rid of the discontinuities of the sectionally constant periodic permittivity $\varepsilon_r(\mathbf{r})$. More specifically, the equations that define the eigensystem in the transformed space must not depend explicitly on $\varepsilon_r(\mathbf{r})$, because otherwise the technique proposed in our previous work is not appropriate to compute the eigenvalues. The solution proposed here (which is an improvement of the results briefly described in Silveirinha and Fernandes [2002]) involves unfolding the

original propagation problem in two related problems defined in homogeneous spaces. Before presenting the details of the formulation, the geometry of the dielectric crystal is described in the next section.

Geometry

The periodic medium is depicted in Figure 1a. It consists of a two-dimensional array of dielectric cylinders with arbitrary cross-section embedded in a dielectric medium with permittivity ε_{r1} (the host medium). The cylinders are oriented along the z-direction and are made of a dielectric material with (relative) permittivity ε_{r2}. It is assumed that the dielectric cylinders are not connected. The medium is invariant to translations along the primitive vectors $\mathbf{a}_1$ and $\mathbf{a}_2$.

As is well known, the propagation problem is intrinsically two-dimensional in the on-plane case. The unit cell Ω is illustrated in Figure 1b. We denote the cross-section of the inclusions by D, and the boundary of the D by ∂D. The outward unit normal vector is $\hat{\mathbf{v}}$.

The objective is to characterize the electromagnetic Floquet modes, i.e., the periodic solutions modulated by the propagation factor $\exp(-j\mathbf{k}.\mathbf{r})$, where $\mathbf{k}$ is the wave vector and $\mathbf{r}$ is a generic point of space. Our analysis is restricted to the on-plane case: i.e., $\mathbf{k}$ is normal to the cylinders. In this situation, the electromagnetic waves decouple into E-polarized waves (transverse magnetic with respect to the z-direction) and H-polarized waves (transverse electric with respect to the z-direction). In addition, the vector problem reduces to a scalar problem characterized by the scalar potential ψ.

We put $\psi = E_z$ in the E-polarization case and $\psi = H_z$ in the H-polarization case (E_z and H_z are, respectively, the electric and magnetic fields along the z-direction). Since the geometry is two-dimensional, the coordinate of space along the z-direction can be discarded, and the observation point and wave vector can be written as $\mathbf{r} = (x_1, x_2)$ and $\mathbf{k} = (k_1, k_2)$, respectively. The scalar potential satisfies the following wave equation:

$$\nabla^2\psi + \varepsilon_r\beta^2\psi = 0, \qquad \text{off the interfaces,} \tag{1}$$

where $\nabla^2 = \partial^2/\partial x_1^2 + \partial^2/\partial x_2^2$, $\beta = \omega/c$ is the free-space wave number, ω is the angular frequency, and c is the velocity of light in vacuum. In addition, $\psi\exp(j\mathbf{k}.\mathbf{r})$ is periodic,

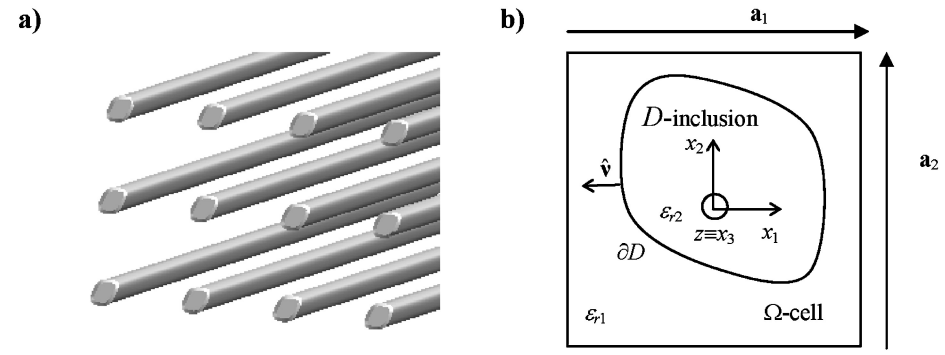

Figure 1. Geometry of the photonic crystals. (a) Fragment of the periodic medium. (b) Cross-section of the unit cell (the medium is intrinsically two-dimensional).

and at the dielectric interfaces, the scalar potential satisfies the boundary conditions:

$$\psi^+ = \psi^-, \frac{1}{\tau_1}\frac{\partial \psi^+}{\psi \mathbf{v}} = \frac{1}{\tau_2}\frac{\partial \psi^-}{\partial \mathbf{v}}, \qquad \text{on the interfaces,} \tag{2}$$

where the superscripts "+" and "−" specify whether the potential is evaluated at the outer or inner side of the interface, $\partial/\partial \mathbf{v}$ is the normal derivative on ∂D, and the constants τ_1 and τ_2 are $\tau_1 = \tau_2 = 1$ in the E-polarization case and $\tau_1 = \varepsilon_{r1}$ and $\tau_2 = \varepsilon_{r2}$ in the H-polarization case.

Since there are no sources, the propagation problem has nontrivial solutions only for specific "resonant" wave numbers $\beta = \beta(\mathbf{k})$ (the eigenvalues of the modal problem). The objective of the paper is to compute the eigenvalues efficiently. For convenience, we denote the set of eigenvalues $\beta = \omega/c$ associated with a given wave vector $\mathbf{k}$ by $\Lambda_{\mathrm{dc}}(\mathbf{k}; \varepsilon_{r1}, \varepsilon_{r2})$. The correspondence $\mathbf{k} \to \Lambda_{\mathrm{dc}}(\mathbf{k}; \varepsilon_{r1}, \varepsilon_{r2})$ defines the band structure of the dielectric crystal.

Equation (2) shows that the scalar potential is continuous in all space. On the other hand, (1) and (2) also show that the first-order derivatives of ψ are discontinuous at the dielectric interfaces in the H-polarization case, whereas only the second-order derivatives are discontinuous in the E-polarization case. This irregular behavior of ψ is the source of the convergence problems of the plane wave method. In the following sections, it is proved that it is possible to circumvent these problems considering a space transformation that improves the regularity of the scalar potential.

Extended Problem

In order to generalize the method proposed in Silveirinha and Fernandes (2003), not only the scalar potential ψ must be regularized, but also the differential operators. In fact, in the dielectric case the operator that acts on ψ, $\nabla^2 + \beta^2 \varepsilon_r$, depends explicitly on $\varepsilon_r(\mathbf{r})$, which is a discontinuous function. This situation does not occur in the metallic case because in that problem we can always assume that ε_r is constant over all space.

In this section, it is explained how the differential operator can be regularized. Our solution is to unfold the propagation problem in two coupled problems defined in homogeneous spaces. The concept is illustrated in Figure 2. The potential ψ defined in the dielectric crystal is unfolded in the potentials ψ_1 and ψ_2. The potential ψ_1 (ψ_2) is defined in a homogeneous space with relative permittivity ε_{r1} (ε_{r2}). The relation between ψ and the auxiliary potentials ψ_1 and ψ_2 is explained next.

Let us suppose that dielectric inclusions are removed from the dielectric crystal. In that case, the medium becomes homogeneous with permittivity ε_{r1}. The scalar potential in the new homogeneous space is by definition ψ_1. We impose that the scalar potential remains unchanged in the host medium, i.e., that $\psi_1 = \psi$ in the host region (the non-shaded region in Figure 2). On the other hand, we consider that the scalar potential is extended to the inner region as a continuous solution of the Helmholtz equation (1), with $\varepsilon_r = \varepsilon_{r1}$ (i.e., ψ_1 is extended to the inner region as a solution of an interior Dirichlet problem).

The definition of ψ_2 is analogous to that of ψ_1: We suppose that the host medium is replaced by a dielectric with the same permittivity as the dielectric cylinders. In this way, the medium becomes homogeneous with permittivity ε_{r2}. The scalar potential in the new homogeneous space is by definition ψ_2. We impose that the scalar potential remains unchanged in the dielectric inclusions, i.e., that $\psi_2 = \psi$ in the inner region.

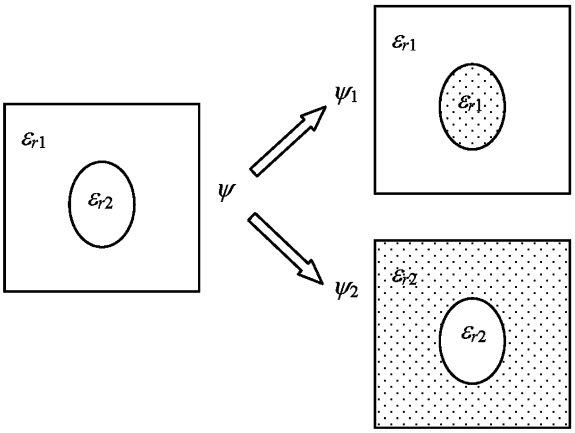

Figure 2. The scalar potential is "unfolded" in two auxiliary potentials defined in homogeneous spaces. The figure depicts the unit cell of the different spaces.

We extend the scalar potential ψ_2 to the outer region as a continuous solution of (1), with $\varepsilon_r = \varepsilon_{r2}$. In doing this there is a degree of freedom. Indeed, it is possible to choose many different boundary conditions on the boundary of the unit cell. For simplicity, Floquet wave boundary conditions are chosen. However, we will not assume that ψ_2 is necessarily associated with the same wave vector as the potential ψ (the reason will be explained later). We consider that ψ_2 is associated with the wave vector $\mathbf{k}_2$, where $\mathbf{k}_2$ can be arbitrarily fixed. Hence, ψ_2 is extended to the outer region as a solution of an exterior Dirichlet problem with Floquet wave boundary conditions.

From the above definitions, it is clear that ψ_1 and ψ_2 satisfy the following formulas:

$$\nabla^2\psi_i + \varepsilon_{r,i}\beta^2\psi_i = 0, \qquad \mathbf{r} \notin \partial D \qquad (i = 1, 2), \tag{3}$$

$$\psi_1^+ = \psi_2^-, \frac{1}{\tau_1}\frac{\partial\psi_1^+}{\partial\mathbf{v}} = \frac{1}{\tau_2}\frac{\partial\psi_2^-}{\partial\mathbf{v}}, \qquad \text{on } \partial D, \tag{4}$$

$$\psi_i \exp(j\mathbf{k}_i.\mathbf{r}) \qquad \text{is periodic} \qquad (i = 1, 2). \tag{5}$$

The superscripts "+" and "−" refer to the outer and inner sides of ∂D, respectively. The coupling condition (4) is a consequence of (2), and of $\psi_1 = \psi$ in the host medium and $\psi_2 = \psi$ in the dielectric inclusions. In (5), we defined $\mathbf{k}_1 = \mathbf{k}$, where $\mathbf{k}$ is the wave vector associated with ψ. As discussed before, the wave vector $\mathbf{k}_2$ can be arbitrarily fixed.

The coupled system formed by (3)–(5) is by definition the "extended problem." Unlike in the original problem, the differential operators that act on ψ_1 and ψ_2 are smooth operators (in the sense that the respective coefficients are smooth functions). In what follows, it will be proved that the extended problem is intrinsically related to the initial problem.

Indeed, the definition of (ψ_1, ψ_2) shows that each nontrivial potential ψ can be associated with a nontrivial solution (ψ_1, ψ_2) of the extended problem.

Reciprocally, let (ψ_1, ψ_2) be an arbitrary continuous solution of the extended problem. This solution can be projected into a solution of the original problem. The projected solution is obviously

$$\psi = \begin{cases} \psi_1 & \text{in the host region,} \\ \psi_2 & \text{in the dielectric inclusions.} \end{cases} \tag{6}$$

Hence, we conclude that there is a correspondence between the solutions of both problems. However, the two problems are not equivalent. Indeed, some solutions of the extended problem can have trivial projection (i.e., the extended problem has more solutions than the original problem). A similar situation occurs in the metallic case, as discussed in Silveirinha and Fernandes (2003).

In fact, the continuous solutions of (3)–(5) either of the type $(\psi_1, 0)$ with $\psi_1 = 0$ in the host region or of the type $(0, \psi_2)$ with $\psi_2 = 0$ in the dielectric inclusions are projected into the trivial solution. The band structure of the extended problem is thus richer than that of the dielectric crystal. More specifically, the band structure of the extended problem contains the band structure of the dielectric crystal, and in addition some bands associated with modes with trivial projection.

Next, we characterize the modes with trivial projection. These modes are the direct sum of internal modes and external modes.

The internal modes are of the type $(\psi_1, 0)$, with $\psi_1 = 0$ in the host region. In this case, the potential ψ_1 can be identified with a Dirichlet mode of a metallic cavity. The metallic cavity has the same cross-section as the cylinders and is filled with a dielectric with permittivity ε_{r1} (notice that ψ_1 is defined in a homogeneous medium with permittivity ε_{r1}). Since ψ_1 vanishes in the host region, it is independent of $\mathbf{k}$. The internal modes are thus dispersionless. Let Λ_{int} be the set of eigenvalues β of the metallic cavity with shape D and normalized (to unity) relative permittivity. Then, the spectrum of the internal modes is $\sqrt{\varepsilon_{r1}}\Lambda_{\text{int}}$.

The external modes are of the type $(0, \psi_2)$, with $\psi_2 = 0$ in the dielectric inclusions. The scalar potential ψ_2 can be identified with an E-polarization Floquet mode in a related metallic crystal (independently of the considered polarization). The metallic crystal is obtained from the initial crystal by replacing the dielectric inclusions by perfect electric conductor (PEC) inclusions, and the host permittivity by ε_{r2}. Therefore, the spectrum of the external modes is $\sqrt{\varepsilon_{r2}}\Lambda_{\text{ext}}(\mathbf{k}_2)$, where $\Lambda_{\text{ext}}(\mathbf{k}_2)$ is the set of eigenvalues β of a metallic crystal with the same topology as the one described above, but normalized (to unity) relative permittivity.

We define $\Lambda_{\text{ep}}(\mathbf{k}; \varepsilon_{r1}, \varepsilon_{r2})$ as the set of eigenvalues of the extended problem. From the previous discussion, there is the following eigenvalue decomposition:

$$\Lambda_{\text{ep}}(\mathbf{k}; \varepsilon_{r1}, \varepsilon_{r2}) = \sqrt{\varepsilon_{r1}}\Lambda_{\text{int}} \cup \sqrt{\varepsilon_{r2}}\Lambda_{\text{ext}}(\mathbf{k}_2) \cup \Lambda_{\text{dc}}(\mathbf{k}; \varepsilon_{r1}, \varepsilon_{r2}). \tag{7}$$

The above formula shows that the eigenfunctions of the extended problem are decomposable into three sets. One of the sets is projected into the eigenfunctions of the dielectric crystal. The other two sets have trivial projection and consist of internal/external modes.

Therefore, we can obtain the eigenvalues of the original problem from the spectrum of the extended problem by extracting the eigenvalues associated with the internal/external modes.

It is important to note that the eigenvalues associated with the internal/external modes are independent of $\mathbf{k}$ (this is the motivation to consider that $\mathbf{k}_2$ is fixed). Therefore, these

eigenvalues are easily detected and extracted from the computed band structure. In fact, they give rise to flat (dispersionless) lines in the computed spectrum. A similar situation occurs in the metallic case (Silveirinha & Fernandes, 2003). More details about this matter will be given later in the article.

Smoothing Map and Eigenvalue Problem

In analogy with the results of our previous paper, the eigenfunctions of the extended problem are mapped into a space of smooth functions where the eigenvalue problem can be solved efficiently.

We use the same smoothing mapping as in Silveirinha and Fernandes (2003). More specifically, the transformation $(\psi_1, \psi_2) \to (\phi_1, \phi_2)$ is defined by:

$$\phi_i(\mathbf{r}) = \psi_i(\mathbf{r}) - \int_{\partial D} f_i(\mathbf{r}')\Phi_p(\mathbf{r}|\mathbf{r}';\mathbf{k}_i)ds', \qquad i = 1, 2, \tag{8a}$$

$$f_i = -\left[\frac{\partial \psi_i}{\partial \mathbf{v}}\right] = \frac{\partial \psi_i^-}{\partial \mathbf{v}} - \frac{\partial \psi_i^+}{\partial \mathbf{v}}, \qquad i = 1, 2, \tag{8b}$$

where $\Phi_p(.;\mathbf{k}_i)$ is the lattice Green function introduced in Silveirinha and Fernandes (2003). Note that the wave vector is shown explicitly in the argument of the Green function. Indeed, both ψ_1 and ψ_2 are Floquet waves, but they are associated with different wave vectors ($\mathbf{k}_1$ and $\mathbf{k}_2$, respectively), as discussed in the previous section. Using the fact that (ψ_1, ψ_2) is continuous and other arguments from our previous paper, it is easy to verify that (ϕ_1, ϕ_2) defined as above is two-times continuously differentiable.

In what follows, an equivalent eigenvalue problem in the ϕ-space is derived. To begin with, we obtain an integral equation for the densities f_1 and f_2 given by (8b). To this end, we let the observation point approach ∂D and we impose the boundary conditions (4). Using the jump conditions (Colton & Kress, 1992), it is found that:

$$\phi_1 + \mathbf{L}_1 f_1 = \phi_2 + \mathbf{L}_2 f_2 \qquad \text{on } \partial D, \tag{9a}$$

$$\frac{1}{\tau_1}\left(\frac{\partial \phi_1}{\partial \mathbf{v}} + \mathbf{M}_{+,1} f_1\right) = \frac{1}{\tau_2}\left(\frac{\partial \phi_2}{\partial \mathbf{v}} + \mathbf{M}_{-,2} f_2\right) \qquad \text{on } \partial D. \tag{9b}$$

In the above, the integral operators $\mathbf{L}_i$, $\mathbf{M}_{+,i}$, and $\mathbf{M}_{-,i}$, $i = 1, 2$, are defined as:

$$\mathbf{L}f = \int_{\partial D} f(\mathbf{r}')\Phi_p(\mathbf{r}|\mathbf{r}')ds', \tag{10a}$$

$$\mathbf{M}_{\pm} f = \int_{\partial D} f(\mathbf{r}')\frac{\partial \Phi_p}{\partial \mathbf{v}}(\mathbf{r}|\mathbf{r}')ds' - \left(\pm\frac{1}{2}f(\mathbf{r})\right), \tag{10b}$$

and the subscript of the operators identifies the wave vector ($\mathbf{k}_i$) associated with the Green function. After straightforward manipulations, it is found that:

$$f_1 = \left(\frac{\mathbf{M}_{+,1}}{\tau_1} - \frac{1}{\tau_2}\mathbf{M}_{-,2}\mathbf{L}_2^{-1}\mathbf{L}_1\right)^{-1}\left(\left(\frac{1}{\tau_2}\frac{\partial \phi_2}{\partial \mathbf{v}} - \frac{1}{\tau_1}\frac{\partial \phi_1}{\partial \mathbf{v}}\right) - \frac{1}{\tau_2}\mathbf{M}_{-,2}\mathbf{L}_2^{-1}(\phi_2 - \phi_1)\right),$$

$$f_2 = \left(\frac{\mathbf{M}_{-,2}}{\tau_2} - \frac{1}{\tau_1}\mathbf{M}_{+,1}\mathbf{L}_1^{-1}\mathbf{L}_2\right)^{-1}\left(-\left(\frac{1}{\tau_2}\frac{\partial \phi_2}{\partial \mathbf{v}} - \frac{1}{\tau_1}\frac{\partial \phi_1}{\partial \mathbf{v}}\right) + \frac{1}{\tau_1}\mathbf{M}_{+,1}\mathbf{L}_1^{-1}(\phi_2 - \phi_1)\right). \tag{11a}$$

The superscript "−1" refers to the inverse of an integral operator. The above formulas show that f_1 and f_2 depend uniquely on (ϕ_1, ϕ_2).

Substituting (8a) in (3) we also find that:

$$\nabla^2\phi_i + \varepsilon_{r,i}\beta^2\left(\phi_i + \int_{\partial D} f_i(\mathbf{r}')\Phi_p(\mathbf{r}|\mathbf{r}';\mathbf{k}_i)ds'\right) = 0 \qquad (i = 1, 2), \tag{11b}$$

$$\phi_i \exp(j\mathbf{k}_i.\mathbf{r}) \qquad \text{is periodic} \qquad (i = 1, 2). \tag{11c}$$

Equation (11) is an integral-differential eigensystem in (ϕ_1, ϕ_2). Our previous analysis shows that the mapping $(\psi_1, \psi_2) \to (\phi_1, \phi_2)$ given by (8) transforms every solution (ψ_1, ψ_2) of the extended problem into a solution (ϕ_1, ϕ_2) of the integral-differential eigensystem. Reciprocally, every solution of the integral-differential eigensystem can be transformed into a solution of the extended problem. The inverse mapping is defined by rearranging the terms in (8a) and (11a). Hence, (11) is equivalent to the extended problem; i.e., both problems have the same eigenvalues.

Since the eigenfunctions of (11) are smoother than the eigenfunctions of the extended problem, the convergence rate of the plane wave method in the transformed space is better than in the initial space. This fact is used to compute the band structure of a dielectric crystal efficiently.

To this end, we expand (ϕ_1, ϕ_2) as follows:

$$\phi_i(\mathbf{r}) = \sum_{\mathbf{J}} c^i_{\mathbf{J}} g_{\mathbf{J}}(\mathbf{r};\mathbf{k}_i) \qquad (i = 1, 2), \tag{12}$$

where $c^1_{\mathbf{J}}$ and $c^2_{\mathbf{J}}$ are the complex coefficients of the plane wave expansion and $g_{\mathbf{J}}$ is the normalized plane wave defined by:

$$g_{\mathbf{J}}(\mathbf{r};\mathbf{k}) = \frac{1}{\sqrt{\mathrm{V}_{\mathrm{cell}}}} e^{-j\mathbf{k}_{\mathbf{J}}.\mathbf{r}}, \qquad \mathbf{k}_{\mathbf{J}} = \mathbf{k} + j_1\mathbf{b}_1 + j_2\mathbf{b}_2, \tag{13}$$

where $\mathrm{V}_{\mathrm{cell}} = |\mathbf{a}_1 \times \mathbf{a}_2|$ is the area of the unit cell, and $\mathbf{b}_1$ and $\mathbf{b}_2$ are the primitive vectors of the reciprocal lattice. These vectors are defined by the relations $\mathbf{a}_n.\mathbf{b}_m = 2\pi\delta_{n,m}$, $n, m = 1, 2$, where $\delta_{n,m}$ is the Kronecker symbol. Note that the wave vector associated with the plane wave depends on the considered potential.

Now, the objective is to obtain a matrix eigensystem in which the eigenvectors are associated with the unknown coefficients $c^i_{\mathbf{J}}$. Inserting (12) into (11b) and proceeding as in Silveirinha and Fernandes (2003), it is easy to obtain that:

$$\frac{\varepsilon_{r,i}}{|\mathbf{k}_{\mathbf{I},i}|^2} c^i_{\mathbf{I}} + \frac{\varepsilon_{r,i}}{|\mathbf{k}_{\mathbf{I},i}|^4} \langle g_{\mathbf{I}}(.;\mathbf{k}_i)|f_i\rangle_{\partial D} = \frac{1}{\beta^2} c^i_{\mathbf{I}}, \qquad i = 1, 2, \tag{14}$$

where $\mathbf{I} = (i_1, i_2)$ is a generic multi-index of integers, and $\mathbf{k}_{\mathbf{I},i} = \mathbf{k}_i + i_1\mathbf{b}_1 + i_2\mathbf{b}_2$.

Equations (11a) and (14) form a standard matrix eigensystem that can be solved numerically. To this end, the integral operators are discretized and the plane wave expansion truncated. The eigenvalues of the matrix eigensystem are $1/\beta^2$ and are coincident with the eigenvalues of the extended problem.

Ahead, we present several numerical examples that prove that the proposed approach may dramatically improve the convergence rate to the standard plane wave method. Before that, in the next section, it is briefly discussed how the band structure of the dielectric crystal can be obtained from the band structure of the extended problem.

Band Structure of the Dielectric Crystal

As proved before, the eigenmodes of the extended problem can be identified either with modes of the dielectric crystal or with internal/external modes with trivial projection. Thus, it is possible to obtain the eigenvalues of the dielectric crystal by extracting the eigenvalues of the extended problem associated with the internal/external modes. The objective of this section is to elucidate how one can recognize if a given eigenvalue is associated with an internal/external mode.

As discussed earlier, the simplest solution is to detect the dispersionless bands in the calculated band structure. This is so because the eigenvalues of the internal/external modes are independent of the wave vector **k**. Hence, if one solves the modal problem many times with different wave vectors (e.g., in band structure calculations) the eigenvalues associated with the internal/external modes are obtained repeatedly and so can be easily identified.

A different approach to identifying the internal/external eigenvalues is to precalculate them (see also our previous article). This can be done in two different ways.

The easiest way is to note that the unwanted eigenvalues are associated with the resonant modes of a related metallic cavity/metallic crystal. Thus, they can be calculated using the method proposed in Silveirinha and Fernandes (2003). This approach is especially appropriate because the associated integral operators are also needed to solve the extended problem (so the additional computational effort is very small). It is important to note that the eigenvalues associated with internal/external modes only need to be calculated once, because they are independent of **k**. Thus, the total effort to compute these eigenvalues is negligible as compared with the effort required to obtain the band structure of a dielectric crystal (which involves solving the propagation problem for many wave vectors).

The second alternative (not so good) is to note that the internal modes of the extended problem are mapped into modes of the form $(\phi_1, 0)$, while the external modes are mapped into modes of the form $(0, \phi_2)$. Therefore, theoretically, it is easy to recognize the internal/external eigenvalues: They are associated with eigenfunctions either of the type $(\phi_1, 0)$ or of the type $(0, \phi_2)$ in the transformed space. We can test if a given eigenvalue β is associated with an internal/external mode by computing the eigenvectors $(c_{\mathbf{I}}^1, c_{\mathbf{I}}^2)$ of the matrix eigensystem (14). The mode is internal if $c_{\mathbf{I}}^2 = 0$ for every $\mathbf{I}$ and is external if $c_{\mathbf{I}}^1 = 0$ for every $\mathbf{I}$. Although theoretically rigorous, this approach is not very attractive in practice due to obvious numerical limitations.

Numerical Simulations

Here, numerical results that validate our theory and demonstrate the efficiency of the proposed approach are presented.

To begin with, we compare the results obtained with our method with other results published in the literature (Villeneuve & Piché, 1992). To this end, we calculated the band structure of a triangular lattice of dielectric cylinders with permittivity $\varepsilon_{r2} = 16$ and volume fraction 35%. The cross-section of the cylinders is circular. The host medium is air, i.e., $\varepsilon_{r1} = 1$. The lattice constant is a.

The numerical results were calculated by solving a 98×98-matrix eigensystem (ϕ_1 and ϕ_2 were expanded with 49 plane waves each). The integral operators were discretized with 32 points on the dielectric interface. The computation time for each wave vector is less than 2 s in a Pentium III-800MHz. In Figure 3, the calculated band structure for the H-polarized waves is depicted. Data extracted from Villeneuve and

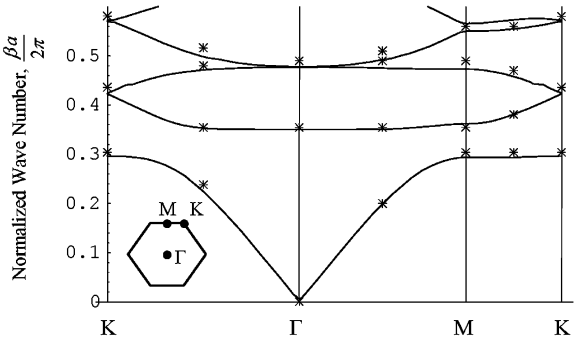

Figure 3. Band structure of the H-polarized waves. The inclusions are circular cylinders with permittivity 16. The volume fraction is 35%. The stars "*" represent results extracted from Villeneuve and Piché (1992).

Piché (1992) ("*"-symbol) is superimposed on the computed results. The agreement is satisfactory, especially for low frequencies. The inset of the figure corresponds to the Brillouin zone of the triangular lattice (Sakoda, 2001). The highly symmetric points Γ, M, and K are also shown.

As seen in Figure 3, the periodic medium has a band gap for H-polarized waves. The band gap between the first and second bands is defined by $0.30 < \beta a/2\pi < 0.35$.

The static effective permittivity associated with the H-polarized waves (calculated from the slope of the fundamental band at the origin) is 1.89. This value is practically independent of the number of plane waves N_p considered in the expansion. The relative difference between the permittivity calculated with $N_p = 18$ and $N_p = 1058$ is as small as $3 \times 10^{-6}\%$. This result anticipates that the convergence rate of the method is very good.

In order to study this matter in detail, we have implemented the standard plane wave method using the algorithm described in Sakoda (2001). In Figure 4, the relative error in the static effective permittivity (for the H-polarization) is depicted as a function of $\sqrt{N_p}$. The reference value is that obtained with our method and $N_p = 1058$ (this corresponds to the limit of the computational resources).

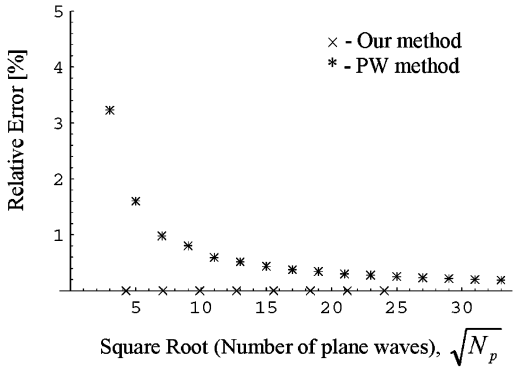

Figure 4. Relative error in the static effective permittivity (in percentage), as a function of the number of plane waves ("*": plane wave method; "×": our method) (H-polarization).

As referred to before, the results calculated with our method are practically independent of N_p. Thus, the corresponding relative error is extremely small. On the other hand, the permittivity obtained with the plane wave method converges very slowly. For $N_p = 33^2 = 1089$, the estimated relative error is 0.19%.

Since the plane wave method converges slowly, it is appropriate to use an extrapolation method to obtain the asymptotic limit of the permittivity as N_p grows to infinity (Sozuer, Haus, & Inguva, 1992). Apparently, the plane wave method converges as $1/\sqrt{N_p}$ (in the two-dimensional case). The extrapolated value for the effective permittivity differs 0.02% from that calculated using the hybrid method. It is estimated that the number of plane waves necessary for an error smaller than 0.1% is $N_p = 5625$. Note that a better result can be obtained with our method using only $N_p = 18$.

The convergence problems of the plane wave method are more serious for high frequencies. To illustrate this aspect we have calculated the relative error in the third eigenvalue at the Γ point. Again, the reference value is that obtained with our method and $N_p = 1058$. The calculated results are depicted in Figure 5. Using our method, the error converges to zero relatively fast. For $\sqrt{N_p} = 7.07$ (i.e., 50 plane waves) the error is about 1%.

On the other hand, the plane wave method converges very slowly. For $N_p = 33^2 = 1089$, the estimated relative error is 2%. The extrapolated value for the eigenvalue differs 0.05% from that obtained using our method. It is estimated that 4225 plane waves are necessary for an error smaller than 1%.

Next, the convergence rate of the E-polarized waves is discussed. The geometry of the periodic medium is the same as before. We computed the relative error in the static effective permittivity (extracted from the slope of the dispersion characteristic).

In the E-polarization case, the static effective permittivity is known in closed analytical form and is equal to the spatial average permittivity. For the considered geometry, it is equal to 6.25. The value obtained with our method agrees excellently with the theoretic value. The relative error is about 10^{-4}% for 18-plane waves.

On the other hand, as depicted in Figure 6, the results obtained with the plane wave method converge slowly. The relative error for $N_p = 33^2 = 1089$ is still 3.96%. The extrapolated value for the effective permittivity differs 0.4% from the theoretical value. It is estimated that 44,100 plane waves are necessary for an error smaller than 2%.

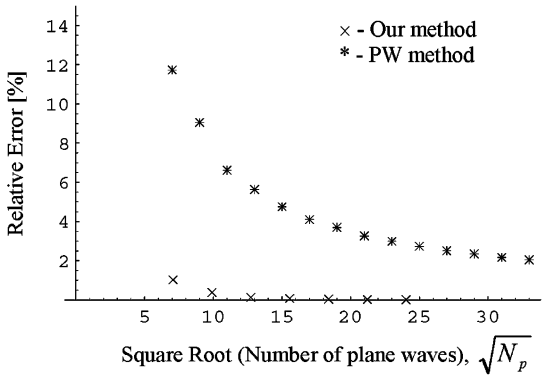

Figure 5. Relative error in the third eigenvalue at the Γ point (in percentage), as a function of the number of plane waves ("*": plane wave method; "×": our method).

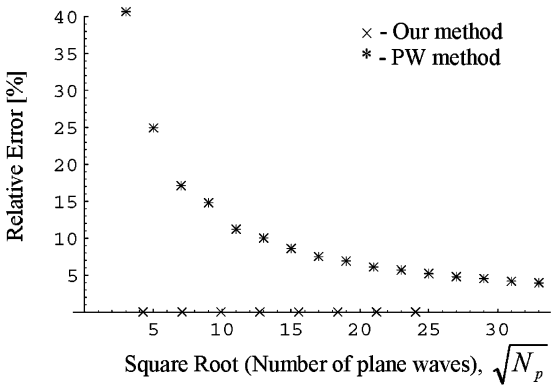

Figure 6. Relative error in the static effective permittivity (in percentage), as a function of the number of plane waves ("*": plane wave method; "×": our method) (E-polarization).

The previous results clearly illustrate the convergence problems of the plane wave method. They also demonstrate that our method yields very accurate results with a moderate number of plane waves.

Conclusions

In this article it was explained how the hybrid method proposed in Silveirinha and Fernandes (2003) can be extended to the dielectric case. The key idea is to map the eigenfunctions of the propagation problem into a space of smooth functions where the plane wave method can be applied with good convergence rate. The main difficulty with the dielectric case is that the regularization of the eigenfunctions is insufficient to improve the convergence rate of the method. Indeed, we also need to regularize the differential operators that act on the electromagnetic modes. As proved in this paper, this can be done by unfolding the propagation problem into two coupled problems defined in homogeneous spaces.

The theoretical work was validated with numerical simulations. The results obtained with our formalism were successfully compared with data extracted from the open literature. In addition, the convergence rate of our method was compared with that of the standard plane wave method. The simulations show that our approach is very accurate and may dramatically improve the efficiency of the standard technique. It was shown that in some examples the computational resources are insufficient for the plane wave method to converge (4% error in the worst case), whereas our method converges very fast and with negligible effort. The typical computation time for each wave vector is less than 2s in a standard personal computer.

References

Colton, D., & R. Kress. 1992. *Inverse acoustic and electromagnetic scattering theory.* Applied Mathematical Sciences 93. Berlin: Springer-Verlag.

Kosaka, H. et al. 1998. Superprism phenomena in photonic crystals. *Phys. Rev. B* 58(10096(R)):1–4.

Luo, C., S. G. Johnson, J. D. Joannopoulos, & J. B. Pendry. 2002. All-angle negative refraction without effective index. *Phys. Rev. B* 65(201104(R)):1–4.

Maagt, P., R. Gonzalo, Y. C. Vardaxoglou, & J. M. Baracco. 2003. Electromagnetic bandgap antennas and components for microwave and (sub)millimeter wave applications. *IEEE Trans. AP* 51(10):2667–2277.

Meade, R. D., K. D. Brommer, A. M. Rapper, & J. D. Joannopoulos. 1991. Photonic bound states in periodic dielectric materials. *Phys. Rev. B* 44:13772.

Meade, R. D., A. M. Rappe, K. D. Brommer, J. D. Joannopoulos, & O. L. Alerhand. 1993. Accurate theoretical analysis of photonic band-gap materials. *Phys. Rev. B* 48:8434.

Sakoda, K. 2001. *Optical properties of photonic crystals.* Springer Series in Optical Sciences 80. Berlin: Springer-Verlag.

Silveirinha, M., & C. A. Fernandes. 2002. A hybrid method for the calculation of the band structure of 2D photonic crystals. *Proc. IEEE APS/URSI Symposium*, San Antonio, TX, USA, Vol. 4, pp. 348–351.

Silveirinha, M., & C. A. Fernandes. 2003. Efficient calculation of the band structure of periodic materials with cylindrical metallic inclusions. *IEEE Trans. Microwave Theory Techniques* 51(5):1460–1466.

Silveirinha, M., & C. A. Fernandes. 2004. A hybrid method for the efficient calculation of the band structure of 3D metallic crystals. *IEEE Trans. Microwave Theory Techniques* 52(3):889–902.

Sozuer, H. S., & J. W. Haus. 1993. Photonic bands: Simple-cubic lattice. *J. Opt. Soc. Amer. B* 10:296.

Sozuer, H. S., J. W. Haus, & R. Inguva. 1992. Photonic bands: Convergence problems with the plane-wave method. *Phys. Rev. B* 45:13962.

Villeneuve, P. R., & M. Piché. 1992. Photonic band gaps in two-dimensional square and hexagonal lattices. *Phys. Rev. B* 46:4969.

Villeneuve, P. R., & M. Piché. 1994. Photonic bandgaps: What is the best numerical representation of periodic structures? *J. Mod. Optics* 41:241–256.

Walker, J. S. 1988. *Fourier analysis.* Oxford: Oxford University Press, pp. 315–319.

Yablonovitch, E. 1987. Inhibited spontaneous emission in solid-state physics and electronics. *Phys. Rev. Lett.* 58:2059.

Yablonovitch, E., T. J. Gmitter, R. D. Meade, A. M. Rappe, K. D. Brommer, & J. D. Joannopoulos. 1991. Donor and acceptor modes in photonic band structure. *Phys. Rev. Lett.* 67:3380.

Yablonovitch, E., T. J. Gmitter, & K. M. Leung. 1991. Photonic band structure: The FCC case employing nonspherical atoms. *Phys. Rev. Lett.* 67:2295.